Journal of the Korean Nuclear Society
Vol. 3, No. 3, September, 1971

≪Original≫ Effects of Amount of Second Cold-Reduction on Secondary Recrystallization and Texture Development in Grain-Oriented Silicon Steel

Young Ku Yoon* and Taek Dong Lee**

Physical Metallurgy Laboratory, Korea Institute of Science & Technology, Seoul, Korea
(Received August 9, 1971)

Abstract

Two laboratory-melt heats of 3.25 silicon-iron were made and processed according to a normal commercial practice. Some of the important processing variables that were studied in relation to secondary recrystallization and texture development were contents of manganese and sulfur, heat-treatments after hot-rolling that were used to achieve different hot-rolled microstructures, and amounts of second cold-reduction. The main effort of the present study was directed toward elucidating the relationships among the amount of second cold-reduction, activation energies associated with secondary recrystallization and texture development.

The specimens that had been cold-reduced 10% exhibited only grain growth by strain-induced grain boundary migration and did not exhibit secondary recrystallization. Secondary recrystallization did not appear to completely occur in the 30% cold-reduced specimens, although the nucleation for secondary recrystallization was observed. The second cold-reduction in an amount of 50% was shown to be the optimun for secondary recrystallization and texture development by subsequent processing.

요 약

3.25% 규소를 함유하는 규소강을 용해·합금하고 압연·열처리하여 연질 자심재료로서 응용범위가 넓은 방향성 규소강판을 제조·실험했다. 이 연구에서는 잉고트 중의 망간 및 유황함량, 탄화물 석출과 유관한 열간압연 직후의 열처리조건, 2차 냉간압연율 등이 2차 재결정 및 집합조직에 미치는 영향을 다루었다. 그 중에서도 특히 2차 냉간압연율이 2차 재결정과 관련한 각종 활성화 에너지와 집합조직에 미치는 영향을 중점적으로 구명하였다.

2차 냉간압연율이 10%인 시편은 응력 변형의 도입으로 인한 결정입계 이동으로 결정립성장 만이 관찰되었으며 핵생성을 동반한 2차 재결정은 일어나지 않았다. 2차 냉간압연율이 30%인 시편에서는 2차 재결정을 위한 핵생성만 있었으며 2차 재결정이 완전히는 일어나지 않았다. 이 실험 조건하에서 50%의 2차 냉간압연율이 2차 재결정을 일으키기에 최적 냉간 압연율이며 가장 높은 직접도를 얻을 수 있는 압연율이었다.

* Young Ku Yoon is presently with the Korean Atomic Energy Research Institute.
** Taek Dong Lee is presently at the Graduate School of New York University.

I. Introduction

Soft magnetic materials are required for the manufacture of electric motors, generators, transmission and distribution transformers, and many other electrical equipment. Important magnetic characteristics of the soft magnetic materials are high permeability, high saturation flux density and low core loss(or total energy loss). Silicon steel containing 0.5% to 4.5% silicon is one of the widely used and best soft magnetic materials that meet the afore-mentioned characteristics.

The historical background, importance, metallurgical factors and magnetic properties of silicon steel have been reviewed previously.[1] As mentioned in the review, silicon steel sheets are classed in two categories; non-oriented and grain-oriented silicon steel, depending on whether there is the (110)[001] texture (or preferred orientation) developed or not. Grain-oriented silicon steel sheets are not produced as yet in Korea. Their production requires a relatively sophisticated technology of steel making, processing and treatment. Final magnetic properties of grain-oriented silicon steel sheets are influenced greatly by metallurgical factors. Namely, the saturation flux density depends on their chemical composition, particularly, silicon content, whereas the permeability, the coercive force and the core loss (strictly speaking, hysteresis loss) are influenced by contents and distribution of impurities, lattice defects, internal stresses and degree of texture development.

The present study concerns effects of contents of manganese and sulfur, hot-rolling conditions and amount of second cold-reduction on secondary recrystallization and texture development, and consequently, final magnetic properties of grain-oriented silicon steel. As regards chemical composition, contents of impurity elements should be kept as low as possible to achieve good magnetiic properties in final silicon steel sheet products.[2] The presence of appropriate second-phase impurities, however, is required for secondary recrystallization and development of a strong texture in silicon steel sheets above a critical high temperature.[3,4] The second-phase impurities are to inhibit the grain growth of primary recrystallized grains and to stabilize the structure up to a certain temperature.

In the present study two ingots having different levels of manganese and sulfur were processed. The impurities have been known to form a second-phase that plays the beneficial role in secondary recrystallization. Since cooling practices after hot-rolling were reported to influence final magnetic properties significantly, various cooling practices were experimented to study their effects on carbide precipitation and texture development. Main efforts of the present study were directed toward studying effects of the amount of second cold-reduction on secondary recrystallization and texture development. The amount of second cold-reduction practiced by U.S. Steel[5] as the optimum for development of the (110)[001] texture is 50% for 0.35 mm thick final products whereas the optimum amount proposed by Akatsu is 25 to 40%.[6] It has been previously reported by Gokyu[7] that it is possible by the use of 15 to 20% cold-reduction and slightly different heat-treatments to achieve equally strong texture and good final magnetic properties. A method for producing good quality grain-oriented silicon steel by repeated cold-reductions of less than 2% and modified processing has been also reported.[8] Since the texture of grain-oriented silicon steel is developed by secondary recrystallization, the relationship between the amount of second cold-

reduction and texture development was investigated in conjunction with the mechanism of secondary recrystallization. To relate to the mechanism of secondary recrystallization, activation energies for nucleation, grain growth and over-all recrystallization were determined and evaluated for specimens that had been cold-reduced in different amounts and then annealed.

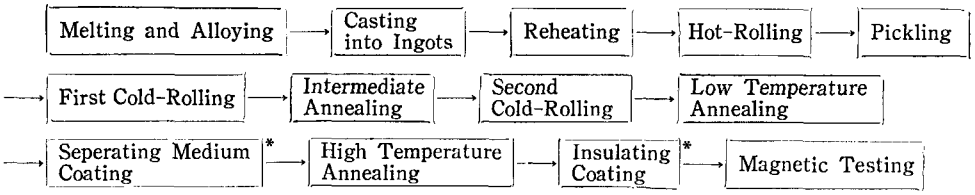

*The processing steps marked with asterisks are not pertinent to the present study and not included in this study.

Fig. 1. Flow sheet of manufacturing process of grain-oriented silicon steel sheets.

II. Materials and Experimental Work

Fig. 1 is a flow sheet of the manufacturing process of grain-oriented silicon steel sheets. Materials and processing conditions used in this study are described in the following.

1. Materials, melting and casting

Melting and alloying were aimed at achieving the chemical composition of grain-oriented silicon steel that is commercially employed by steel producers. For raw materials, industrial pure iron, metallic silicon(J I S No. 1 grade) and electrolytic manganese were used. Additions of sulfur and carbon were made by the use of high purity iron sulfide and high purity carbon. A high frequency induction melting furnace (Ajax Magnethermic Model MCG 50-10 I; 10 kilocycles/second frequency) was used in melting and alloying the silicon steel composition under an argon atmosphere. Alundum crucibles of the ten pound capacity were used for melting. The size of ingots made was 15 to 20 mm in thickness, 60 to 70 mm in width and 200 to 250 mm in length. Table 1 shows the chemical compositions of the ingots. The silicon and phosphor contents of ingots A nad B were almost the same but the sulfur, manganese and carbon contents of the two ingots were quite different. Although the carbon contents were different, both were in a range in which the carbon content does not affect significantly final manetic properties. The manganese and sulfur contents of ingot A were very close to their aimed values but those of ingot B were much lower than the aimed values.

Table 1. Chemical composotions of ingots

Unit: weight %

component / ingot	Si	Mn	S	C	P	Ee
A	3.24	0.088	0.024	0.029	0.01	Balance
B	3.19	0.045	0.019	0.040	0.01	Balance

2. Hot-rolling and subsequent cooling methods.

The ingots of 15 to 20 mm in thickness were reheated to 1300°C and were hot-rolled to 2 mm thick plates. The finishing temperature of hot-rolling, was kept not lower than 800°C. Immediately after hot-rolling, various subsequent cooling methods were applied to study the mode of carbide precipitation. In the present study, the hot-rolled specimens were quenched from the finishing temperature to room temperature and then were reheated to and held at appropriate aging temperatures in the range of 300 to 700°C instead of quenching directly to the aging temperatures. For this experiment the

specimens of the hot-rolled sheets were sealed in evacuated fused-silica capsules and heated to 1300°C for 30 minutes. After breaking the capsules, the specimens were air cooled to a temperature in the range of 800 to 1.00°C and were immediately quenched to room temperature. Some of the quenched specimens were aged for a few minutes at temperatures in the range of 600 to 700°C and the others were aged at temperatures in the range of 400 to 600°C. Both hot and cold-rolling were performed with a two-high reversing-type Stanat rolling mill (roll diameter of 150 mm, roll width of 200 mm).

3. Cold-rolling, annealing and determination of texture development.

After hot-rolling the sheets were first cold-rolled and were given an intermediate anneal for 30 minutes at 870°C in a non-oxidizing atmosphere. The amount of first cold-rolling was controlled from 65 to 80% so that final gage of the sheets would be 0.35 mm in all cases after second cold-rolling of 10%, 30% and 50%. The second cold-rolling was followed by low temperature and high temperature annealing. The low temperature annealing was given for 30. minutes at 800°C in a mixed atmosphere consisting of 86% nitrogen, 12% hydrogen and 2% water vapor (dew point 18°C). During this low temperature annealing, primary recrystallization and decarburization were occured. The high temperature annealing was given by isothermal heating at three different temperatures, 1000°C, 1040°C and 1080°C in a dry hydrogen atmosphere. Secondary recrystallization was achieved during the high temperature annealing.

The degree of texture development in a recrystallized specimen was determined by a

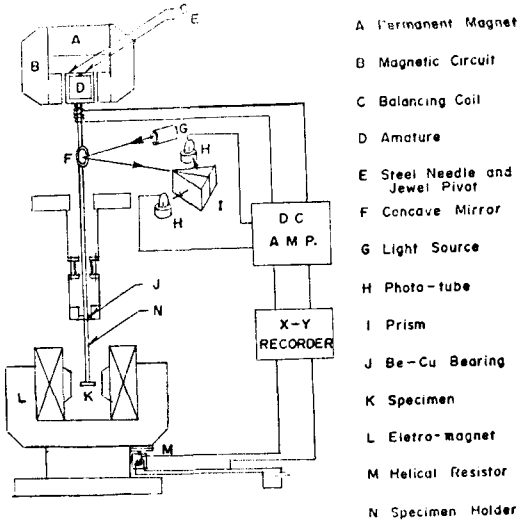

Fig. 2. Schematic diagram showing the principle and construction of the torque magnetometer.

torque magnetometer*, Model TRT-IIB of Toei Industry Inc.. Fig. 2 shows the principle and construction of the torque magnetometer.

The operating principle of this instrument is as follows: A specimen in a disc form, 20 mm in diameter, is attached to the specimen holder and is placed horizontally in the center of a constant magnetic field of appoximately 4000 oersteds. When the field is rotated slowly by rotating the megnet, the torque required to align the easy magnetization direction of the specimen with the field direction is different according to the magnetic anisotropy of the specimen. This torque is amplified and recorded on an X-Y recorder. The degree of texture development is determined by comparing the maximum torque value of the specimen with that of a single crystal of silicon iron. After the measurement of the magnetic torque curves the microstructure of the specimen was examined.

4. Calculation of activation energies

Various activation energies for secondary recrystallization of the second cold-rolled

*The kind and degree of texture development are generally determined by the X-ray pole figure method. When the kinds of texture are known and grain size is large, however, it is more convenient to use the torque magnetometer for a quantitative determination of the degree of texture development.

specimens were calculated by the following method. According to the absolute reaction theory, the specific reaction rate constant k can be expressed as

$$k=A\ \exp(-\Delta H/RT)$$

or $$\ln k=\ln A-\Delta H/RT$$

where R is the gas constant, T is absolute temperature, A is a constant, and ΔH is an activation energy. This equation shows that In k is proportional to 1/T, the slope being $-\Delta$H/R. The activation energy ΔH can be calculated from the slope. In this study the activation energies for nucleation and over-all recrystallization were calculated from the relationship between In k and 1/T at various temperatures by substituting for k reciprocal incubation period, t, in the above equation. The activation energy for grain growth was calculated from the relationship between ln G and 1/T at various temperatures by substituting for k the growth rate of recrystallized grain, G.

III. Experimental Results and Discussion

1. Effects of contents of manganese and sulfur

Since the heats were melted under an argon atmosphere to prevent oxidation during the melting, compounds of the silicon oxide system were scarcely formed. The silcon oxide compounds have high melting points and require long time to rise up to the surface during solidification. The silicon oxide inclusions, if they exist in the ingots, have detrimental effects on final magnetic properties of the products.

Effects of the chemical composition on magnetic properties are generally known: the lower the impurity content of the final products, the better the magnetic properties. During the processing of grain-oriented silcon steel, however, appropriate second phase impurities should be present in adequate amounts to stabilize the primary recrystallized structure below a certain temperature[3,4]. The second phase impurities go into solution, and secondary recrystallization occurs during high-temperature annealing. The impurities that inhibit the grain growth of primary recrystallized grains should be removed after secondary recrystallization.

The second-phase impurity used in this study was manganese sulfide, MnS, and effects of the contents of manganese and sulfur were investigated.

As compared in Table 1, ingot A has 0.088 % manganese and 0.024% sulfur, whereas ingot B has 0.045% manganese and 0.019% sulfur. After the two ingots were fully processed under identical rolling and heat-treating conditions, ingot A showed a higher degree of texture development. Although this data is too limited to draw a conclusion, this result is in agreement with that of U. S. Steel Co.[5] that the optimum contents of manganese and sulfur to obtain good final magnetic properties are 0.08% manganese and 0.025% sulfur.

2. Effects of cooling practices after hot-rolling

Different cooling practices of the specimens heated above the Ae_1 temperature immediately after hot rolling affected significantly the mode of carbide precipitation. When a specimen heated above 800°C was quenched to room temperature and was aged for 1 to 3 minutes at 650°C, grain boundary carbides were precipitated along grain boundaries. The grain-boundary carbides are known as stable cementite, Fe_3C. When a specimen quenched similarly was aged for 1 to 3 minutes at a temperature in the range of 400 to 550°C, however, needle-like carbides were precipitated

on the {100} planes of grains as shown in Fig. 3.

The needle-like carbides are of a metastable carbide and is called as lenticular carbides because they appear in a lens shape under a high magnification microscope. When the specimen was aged for a long time at this temperature, the needle-like carbides broke up into fine dot-like carbides, and the carbon re-precipitated as Fe_3C at grain boundaries. In the specimen aged at 300°C very fine carbides were precipitated. The specimen as quenched, however, showed no carbide precipitate. The precipitation of carbides after the cooling and aging treatments is illustrated in Fig. 4.

It is known that there exists a close correlation between carbide precipitation and final magnetic properties of silicon steel. The presence of the precipitates called lenticular carbides in the hot-rolled strip correlated well with good magnetic properties of the final product. The absence of carbide precipitates indicated an intermediate level of magnetic properties. Conversely, the presence of grain boundary carbides in the hot-rolled strip correlated with poor final magnetic properties.

In order to achieve good magnetic properties, it is, therefore, recommended that the following cooling practice after hot-rolling be used to produce lenticular carbides in the hot-rolled microstructure: Hot-rolling is finished above 800°C and is followed by quenching to 400°C to 500°C by water-spraying and aging for an appropriate time at this temperatue range.

3. Effects of the amount of second cold-reduction on activation energies associated with secondary recrystallization

The amount of second cold-reduction influences texture development and consequently, final magnetic properties of grain-oriented silicon steel. Texture development is achieved by secondary recrystallization that involves nucleation and grain growth. Mechanisms of nucleation and grain growth accompanying second recrystallization in silicon steel has been reviewed previously[1]. Activation energies for nucleation, grain growth and over-all recrystallization were determined for different amounts of second cold-reduction to relate them with the mechanism of secondary recrystallization and texture development.

A. The activation energy for nucleation

As mentioned in the preceding section, the activation energy for nucleation was calculated from the measurements of incubation periods (or induction periods) for nucleation at three different annealing temperatures. The incubation period is interpreted as the period required for nucleation and depends on the solubility and diffusion rate of second phase impurities and the amount of second cold-reduction. The secondary recrystallization process can be divided into nucleation and grain growth stages The delineation of the two stages is somewhat arbitrary. In the present study the incubation period for nucleation was taken as the annealing time required to reach a maximum torque value of 4×10^4 erg/cm^3 for convenience. After the incubation period about 5% of the microstructure was recrystallized in both 50% and 30% cold-reduced specimens. In the 10% cold-reduced specimen 8 to 10% of the microstructure exhibited strain-induced grain-growth that will be further discussed later. Figs. 5, 6 and 7 show the plots of the logarithms of the reciprocal incubation periods for nucleation against the reciprocal annealing temperatures for the cases of 10%, 30% and 50% second cold-reductions, respectively.

The activation energies for nucleation determined from the plots were 65 kcal/mol for the 10% second cold-reduced specimens,

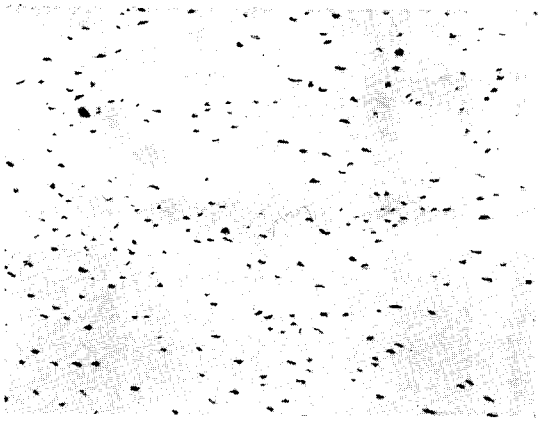

Fig. 3. Microstructure showing lenticular cabides in the specimen quenched from about 800°C to 530°C and aged for 2 minutes at 530°C.

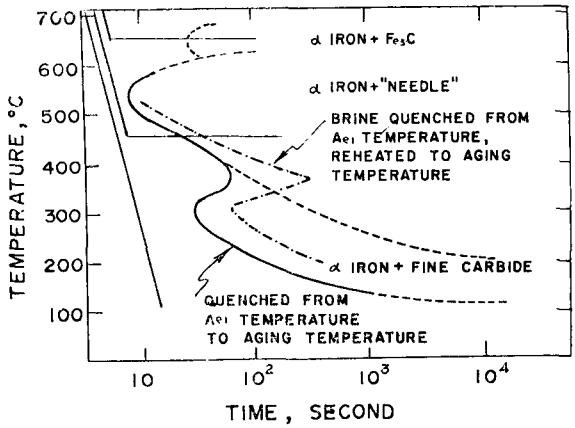

Fig. 4. Precipitation of carbides according to cooling practices in silicon ferrite.

61 kcal/mol for the 30% second cold-reduced specimens and 71 kcal/mol for the 50% second cold-reduced specimens, respectively.

Figs. 8 and 9 show the microstructure of the 10% and 50% second cold-reduced specimens annealed for 30 minutes at 800°C

Fig. 9 shows that the 50% second cold-reduced specimen is recrystallized sufficiently and exhibits a fine grained structure after the low temperature annealing. The microstructure of the 10% second cold-reduced specimen shown in Fig. 8 exhibits much larger grains than the microstructure of the 50% second cold-reduced specimen shown in Fig. 9. This is interpreted as follows: Since the former specimen had been severely reduced as much

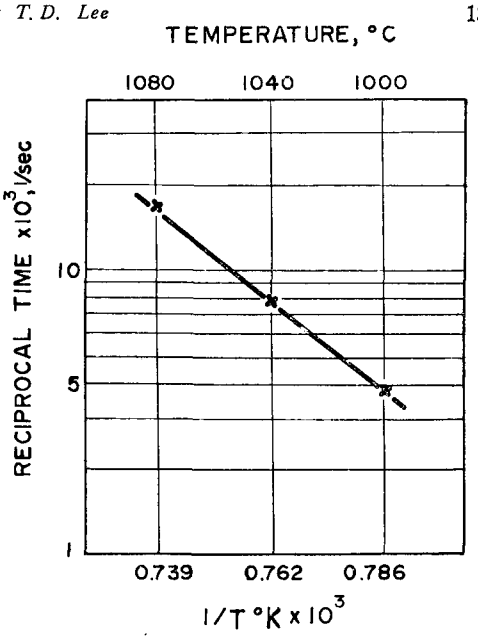

Fig. 5. Plot of the incubation period required to reach a maximum torque value of 4×10^4 erg/cm^3 against annealing temperature in the 10% second cold-reduced specimen

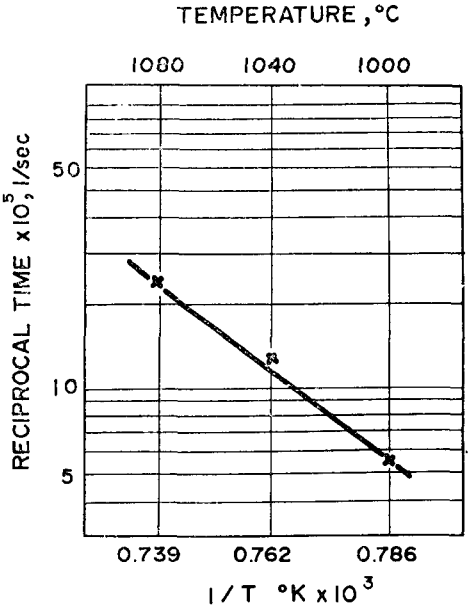

Fig. 6. Plot of the incubation period required to reach a maximum torque value of 4×10^4 erg/cm^3 against annealing temperature in the specimen of 30% second cold-reduced specimen.

as 80% for first cold-rolling, this specimen had a fine-grained structure by recrystallization during the subsequent intermediate annealing at 870°C. The fine grained specimen was

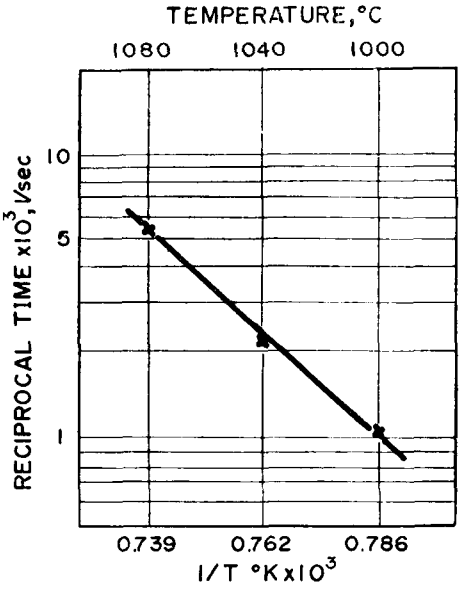

Fig. 7. Plot of the incubation period required to reach a maximum torque value of 4×10^4 erg/cm^3 against annealing temperature in the 50% second cold-reduced specimen.

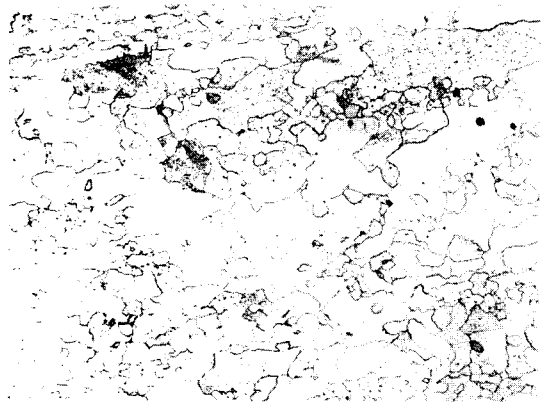

Fig. 8. Microstructure of the 10% second cold-reduced specimen after low temperature annealig. Nital etch; magnification 80X

slightly (10%)reduced for second cold-rolling. During the low temperature annealing, strain-induced grain-growth occurred in the slightly cold-reduced specimen. Figs. 10 and 11 show the microstructure of the 10% and 50% second cold-reduced specimens when they exhibited the maximum torque value of 4×10^4 erg/cm^3 after the low temperature annealing.

It can be observed that large grains were formed by nucleation in the 50% second cold-

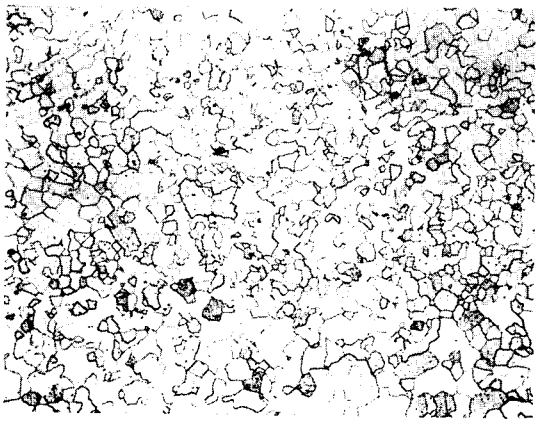

Fig. 9. Microstructure of the 50% second cold-reduced specimen after low temperature annealing. Nital etch; magnification 30X

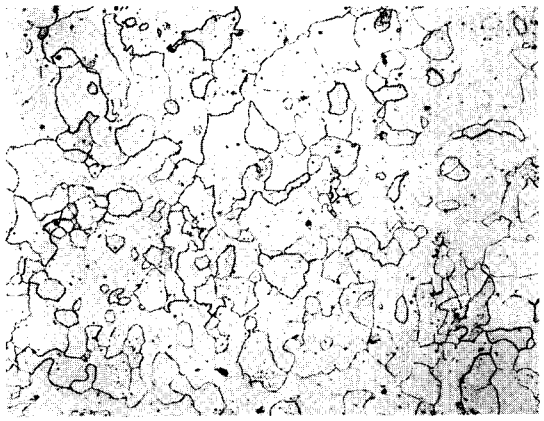

Fig. 10. Microstructure of the 10% second cold-reduced specimen exhibiting a maximum torque value of 4×10^4 erg/cm^3. Nital etch; magnification 30X

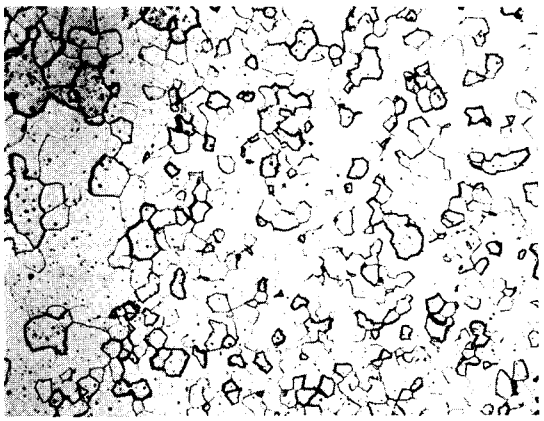

Fig. 11. Microstructure of the 50% second cold-reduced specimen exhibiting a maximum torque value of 4×10^4 erg/cm^3. Nital etch; Magnification 30X

reduced specimen, whereas most grains underwent grain growth to similar sizes in the 10% second cold-reduced specimen. In the case of the 10% second cold-reduced specimen, grain growth occurred by strain-induced grain-boundary migration as already mentioned. The strain-induced grain-growth was reported to occur in 2 to 8% second cold-reduced specimens upon annealing. Since the grains of the 10% second cold-reduced specimen are too large to be recrystallized, secondary recrystallization accompanying nucleation cannot be expected to occur in the specimen.

B. The activation energy for grain growth

After the incubation period, nuclei grow more rapidly than other primary recrystallized grains. For measurement of the the rate of grain growth, many specimens that had been second cold-reduced in same amounts were annealed in a batch, and several of them were drawn from the annealing furnace at appropriate time intervals for microscopic examinations. The rate of grain growth was then determined by measuring the average diameter of largest grains at appropriate time intervals under the microscope. Figs. 12 and 13 show the plots of the logarithm of the rate of grain growth against reciprocal annealing temperature in the 10% and 50% second cold-reduced specimens.

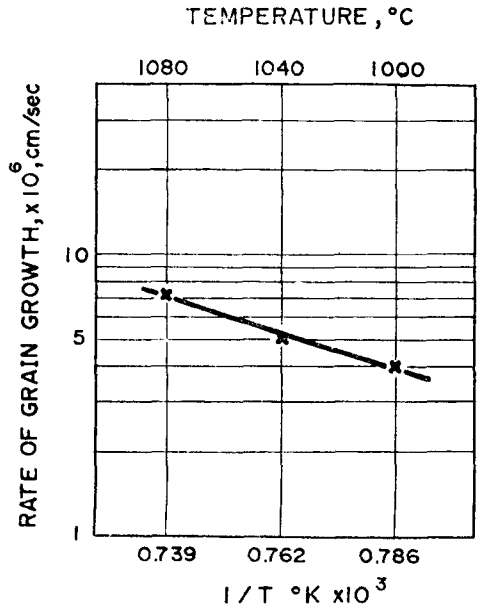

Fig. 12. Plot of the grain-growth rate against annealing time in the 10% second cold-reduced specimen.

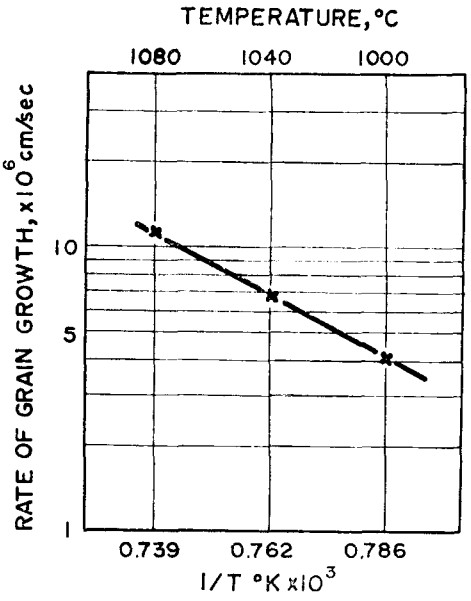

Fig. 13. Plot of the grain-growth rate against annealing time in the 50% second cold-reduced specimen.

Activation energies for grain growth determined from these plots were 30 kcal/mol for the case of the 10% second cold-reduced specimen and 44 kcal/mol for the 50% second cold-reduced specimen. The grain growth of secondary recrystallized grains in the 30% cold-reduced specimen was too small to measure, and the activation energy for grain growth could not be calculated for this case.

C. The activation energy for over-all recrystallization

The activation energy for over-all recrystallization was determined by measuring the annealing time required to reach a fixed amount of recrystallization without delineating between nucleation and grain growth. This activation energy for over-all recrystallization was compared with the activation energies for

nucleation and grain growth. In the present study the annealing time required to achieve a maximum torque value of 6×10^4 erg/cm^3 was taken for convenience as that required to reach a fixed amount of recrystallization. Microscopic examinations of the microstructure of the specimens exhibiting the torque value showed that 35% of the microstructure had undergone recrystallization in the 50% second cold-reduced specimen whereas 80% of the microstructure had undergone recrystallization in the 10% second cold-reduced specimen.

Figs. 14 and 15 show the plots of the logarithm of the annealing time required to achieve the torque value against reciprocal annealing temperature in the 10% and 50% second cold-reduced specimens.

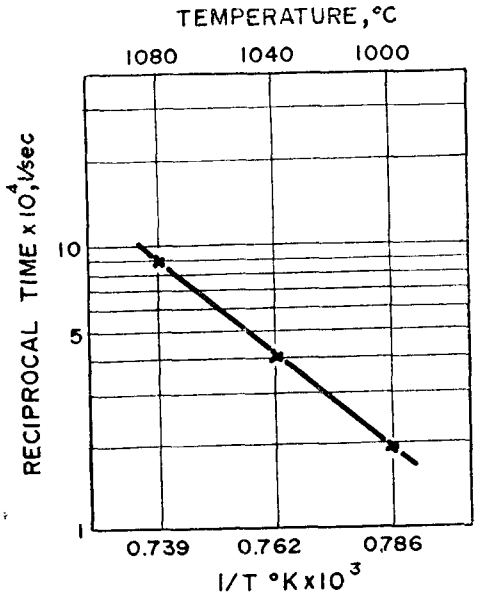

Fig. 14. Plot of the annealing time required to reach a maximum torque value of 6×10^4 erg/cm^3 against annealing temperature in the 10% second cold-reduced specimen.

The activation energies for over-all recrystallization determined from the plots were 67 kcal/mol for the 10% cold-reduced specimen and 49 kcal/mol for the 50% cold-reduced specimen.

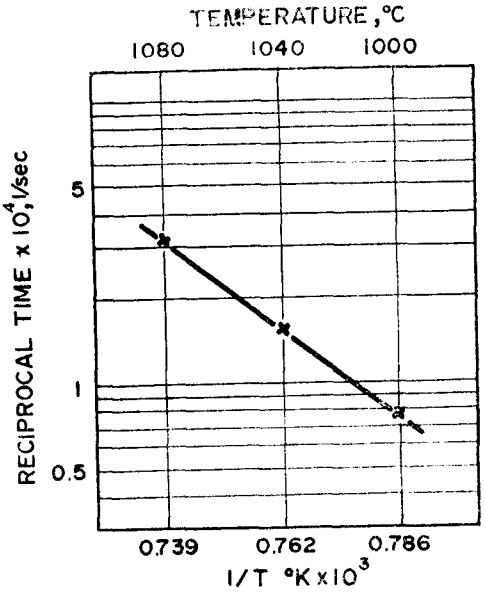

Fig. 15. Polt of the annealing time rebuired to reach a maximum torque value of 6×10^4 erg/cm^3 against annealing temperature in the 50% second cold-reduced specimen

D. Effects of the amount of second cold-reduction on secondary recrystallization and texture developmment

The various activation energies determined as in the preceding sections are summarized in Table 2 to study effects of the amount of second cold-reduction on the activation energies associated with secondary recrystallization.

Table 2. Various activation energies versus the amount of second cold-reduction

Unit: kcal/mol

amount of second cold-reduction	activation energy for nucleation	activation energy for grain growth	activation energy for over-all recrystallization
10%	65*	30	67
30%	61	—	—
50%	73	44	49

*In the 10% second cold-reduced specimen, secondary recrystallization accompanying nucleation was not observed. This value, therefore, signifies an activation energy for grain growth at the early stage and not an activation energy for nucleation.

It can be seen from Table 2 that the activation energies for nucleation are higher than the activation energies for grain growth. This means that nucleation is inhibited by second phase impurities, and primary recrystallized grains have to overcome a certain energy barrier to grow as nuclei The following relationship among the activation energies for nucleation, grain growth and over-all recrystallization was established by Anderson and Mehl[10] ;

$$Q_R = \frac{Q_N + 3Q_G}{4}$$

where Q_R is the activation energy for over-all recrystallization, Q_N is the activation energy for nucleation, and Q_G is the activation energy for grain growth. The activation energies for over-all recrystallization calculated with use of the above equation were 39 kcal/mol for the 10% second cold-reduced specimen and 51 kcal/mol for the 50% second cold-reduced specimen. Comparing these calculated values with the measured values in this experiment, they are in good agreement for the case of the 50% second cold-reduced specimen. For the case of the 10% second cold-reduced specimen, there exists a wide difference between the two values. This means that in this case only grain growth occurred by strain-induced grain boundary migration and not by secondary recrystallization accompanying nucleation and grain growth. Consequently, the above-mentioned equation is not applicable for the case of the 10% second cold-reduced specimen.

Philip and Lenhart[11] studied secondary recrystallization in commercial silicon steel and reported that the activation energy for nucleation was 103 kcal/mol, and the activation energy for grain growth was 103 kcal/mol, and the activation energy for grain growth was 75.5 kcal/mol. Saito[12] also reported that the activation energies were found to vary greatly according to the kind and contents of second phase impurities, and the activation energy for nucleation was in the range of 57 to 135 kcal/mol and the activation energy for grain growth at 900°C was 30 kcal/mol. Since the processing variables and the amount of second cold-reduction were not specified in both reports, it is not possible to compare their results directly with the present results. The activation energies determined in the present study, however, lie in the range of the Saito's results but are lower than the results of Philip and Lenhart. The difference may be attributed to the differences in processing treatments and the kind and contents of second-phase impurities of the materials investigated.

The activation energy for over-all recrystallization is lower for the case of 50% second cold-reduced specimen than for the case of the 10% second cold-reduced specimen. The 50% second cold-reduced specimen also showed the highest degree of texture development. Although the growth rate at the early stage was relatively high for the case of the 10% second cold-reduced specimen, the growth rate soon decreased by grain boundary impingement with other grains. The 10% second cold-reduced specimen exhibited a low maximum torque value after the high temperature annealing. This means that in this specimen many grains having orientations other than the(110)[001] orientation grew. This was observed by the etch-pit technique during the microscopic examinations. Accordingly, it was concluded that the second cold-reduction of 50% has optimum effects on secondary recrystallization and the degree of the (110)[001] texture development.

IV. Summary

1. The ingot containing 0.088% manganese and 0.024% sulfur exhibited a higher degree of texture development and, consequently, better

final magnetic properties than the ingot containing 0.045% manganese and 0.019% sulfur after identical processing.

2. *Lenticular carbides(or needle-like carbides)* were precipitated within grains when the hot-rolled specimen is quenched from a temperature above 800°C to a temperature in the range of 400°C to 500°C and is aged at this temperature range immediately after hot-rolling. The hot-rolled specimen so treated to produce lenticular carbides in the microstructure exhibited better magnetic properties after full processing.

3. When the specimen that had given the second cold-reduction of 10% was annealed, grain growth occurred by strain-induced grain-boundary migration, and secondary recrystallization was not observed. The (110)[001] texture was not well developed. The activation energy for grain growth to reach a maximum torque value of 6×10^4 erg/cm^3 that is equivalent to an activation energy for over-all recrystallization was 67 kcal/mol.

4. For the case of the 30% second cold-reduced specimen, the activation energy for nucleation was 61 kcal/mol. Grain growth did not occur, however, although the specimen was annealed for 2 to 3 hours at 1000°C and 1040°C. No secondary recrystallization was observed.

5. For the case of the 50% second cold-reduced specimen, secondary recrystallization occurred distinctly by the process of nucleation and grain growth. The activation energies for nucleation, grain growth and over-all recrystallization were 73 kcal/mol, 44 kcal/mol and 49 kcal/mol, respectively. The second cold-reduction of 50% was found to be optimum in comparison with the second cold-reduction of 10% and 30%, because the activation energies for over all recrystallization was lowest and the (110)[001] texture was best developed for the former case.

Acknowledgement

This paper is extracted from a thesis in partial fulfillment of the requirements for the M.S. degree at the Graduate School of Seoul National University. The authors wish to express their thanks to Prof. Pyung Choo Park of the College of Engineering, Seoul National University for his helpful discussions and suggestions. The authors are also grateful for the financial support of the Korea Institute of Science & Thechnology.

References

1) Y.K. Yoon, T.D. Lee, Journal of the Korean Institute of Metals., **6**, 192 (1968)
2) R.M.. Bozorth Ferromagnetism, p. 83-87, Van Nostrand, New York (1951)
3) J.D. Fast, Philips Research Reports., **11**, 490 (1956)
4) J.E. May, D. Turnbull, Trans. AIME, 212, 769 (1958)
5) U.S. Steel's Applied Research Laboratory, Private Communication
6) S. Akatsu; Japan Pat. 33-5705
7) I. Gokyu, H. Abe, Y. Nakagawa, Sogoshikenjo-Nenpo, **20**, 42 (1962)
8) Armco Int. Corp, Japan Pat. 193507
9) U.S. Steel Corp, Japan Pat. 38-14009
10) W.A. Anderson, R.F. Mehl, Trans. AIME, **161**, 140 (1945)
11) T.V. Philip, R.E. Lenhart, Trans. AIME, **221**, 439 (1961)
12) T. Saito, Nippon Kinzoku Gakkai-Si, **27**, 191 (1963)